

Nanolubrication studied by Contact-Mode Atomic Force Microscopy

R. Buzio[*,1,2], and **U. Valbusa**[1,2]

[1]Nanomed Labs, Advanced Biotechnology Center, L.go R. Benzi 10, 16146 Genova, Italy
[2]Physics Department, Università degli Studi di Genova, Via Dodecaneso 33, 16146 Genova, Italy

Atomic force microscopy represents a well-established technique for measuring normal and friction forces at the nanoscale. Systematic investigations on the load and velocity dependence of friction loops give access to a new phenomenology, that only partially relies on continuum mechanics theories. We provide a summary of well-established facts and concepts in nanoscale friction phenomena and illustrate novel knowledge emerging in the field of nanolubrication.

Keywords Atomic Force Microscopy; Friction Forces; Nanolubrication

1. Introduction

Friction phenomena deserve prominent attention from the scientific community and considerable efforts are underway to build up a new conceptual framework allowing to understand, and hopefully predict, tribological effects. Nanotribology concerns investigations on friction forces and energy dissipation at the nanoscale: a considerable interest boosts this field, motivated by the perception that it might provide deeper insight into bodies' interactions mechanisms at all length scales, and overcome practice and empiricism that are still dominating friction studies in academic research and traditional manufacturing industries.

The mainstream of nanotribology research focuses on the characterization of dissipation channels involved in single-atoms and multi-atoms sliding contacts, i.e. phonons and electron-hole pairs excitations, adhesion hysteresis, viscoelasticity, generation of lattice defects, plasticity and wear. Experiments and theories usually concern highly idealized model systems, but important contributions often come from broad - apparently unrelated - topics of surface science and (nano)biotechnology: to name a few, design and development of molecular engines, biopolymers mechanics and single-molecule recognition events, biological attachment pads, technological issues in nanoparticles self-assembling, soft lithography techniques, development of scanning probe microscopies with atomic-scale contrast, physical basis for manipulation of single atoms and molecules, nanoscale liquid rheology, microfluidic and microreactors. This observation underlines the fact that nanotribology deals with crucial aspects of mechanical interactions, having deep and generalized implications.

From the experimental point of view, nanotribology achievements strongly rely on the use of the Atomic Force Microscope (AFM): it consists of a nanometer sharp tip dragged over sample surface while accurately monitoring interaction forces; notably it can operate under different environments, from laboratory air or controlled atmosphere to liquid and ultra-high-vacuum, displaying unexpected flexibility and power.

The goal of the present chapter is to summarize the basic principles of friction measurements by AFM and highlight novel knowledge emerging in the field of liquid-mediated nanolubrication.

[*] Corresponding author: e-mail: buzio@fisica.unige.it, Phone: +39 0105737470

2. Basic Principles

The AFM exploits the interaction of a cantilever with a microfabricated tip and the target substrate to reproduce its surface topography and provide information on local properties such as elasticity, hardness, adhesion, surface energy, surface charges, electric and thermal conductivity, electric and magnetic polarizability, optical reflectivity and of course friction. Provided that the tip or the sample are scanned one relative to the other by means of a piezoelectric actuator, the normal and torsional deflections of the cantilever are measured with different techniques in order to map two-dimensional variations of physical quantities with nanoscale accuracy. Since its invention in 1986 [1] the AFM has rapidly evolved in terms of instrumental design and operating principles and the reader is strongly encouraged to read monographies, books and review articles devoted to the subject [2-7]. On the contrary we will focus here on the AFM properties that are of significant interest for nanotribology investigations, particularly on Contact-mode AFM (C-AFM).

In C-AFM the cantilever tip remains in permanent contact with the sample surface while being pulled over it at constant velocity. Maps of torsional lever deflection are acquired simultaneously to topographic information and related to the frictional force acting at the tip apex during sliding: in detail friction force F_f is plotted against tip (or sample) displacement operated in the forward and backward directions along a given scan line, leading to an hysteretic graph (the friction loop) whose average amplitude provides an estimate of the local friction force. Systematic measurements of friction loops amplitude vs normal load F_n and sliding velocity V represent the currently-established protocol for studying friction response at the nanometer scale (for further details see [8,9]). In such context the AFM is also called Scanning Force Microscope, Lateral Force Microscope or Friction Force Microscope; this method mimics macroscale sliding friction measurements, therefore it is the most popular in nanotribology.

3. Nanoscale Friction Phenomenology

3.1 Load Dependence of Nanoscale Friction

The contact mechanics of a nanometric C-AFM probe sliding over nominally-flat surfaces under wearless, purely elastic, dry conditions is subject of extensive investigations yet we are still far to provide a comprehensive picture of this process. In several cases a non-linear relationship is found between friction force and external load, accompanied by the occurrence of a finite friction even at zero or negative (tensile) load. In Fig. 1 we report AFM friction curves showing the typical response of adhesive junctions [10].

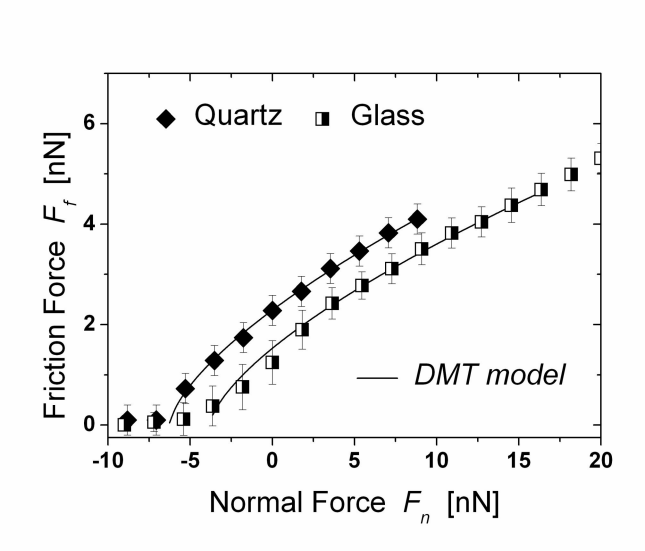

Fig. 1 Average friction vs load curves acquired on quartz and glass surfaces in a low-humidity air atmosphere: they follow a power-law relationship, in agreement with continuum DMT theory and MD simulations (see text). A negative tensile force has to be applied to partially compensate adhesive forces and reduce friction. (adapted from [10]).

The non-linear relationship existing between the normal load F_n and the friction force F_f is usually traced back to a non-linear dependence of the real contact area A_r on the compressive and adhesive forces, F_n and F_{adh}, that is $A_r = A_r(F_n, F_{adh})$: the latter is predicted by continuum contact mechanics models dealing with a sphere-on-flat geometry [11]. It can be simply assumed:

$$F_f = \tau \cdot A_r \tag{1}$$

where τ is a load-independent shear stress. Equation (1) represents a key assumption in experimental nanotribology, being extensively used to analyse C-AFM experiments on bare solid surfaces in ultra high vacuum, controlled atmosphere and ambient air. Continuum models for spherical bodies predict the Hertzian scaling $A_r \approx F_{eff}^{2/3}$, where the effective normal force F_{eff} depends F_n and F_{adh} according to a functional relationship $F_{eff} = F_{eff}(F_n, F_{adh})$. Two well-known models, the Johnson-Kendall-Roberts (JKR) theory [12] and the Derjaguin-Muller-Toporov (DMT) theory [13], describe the contact mechanics of single junctions respectively for compliant and stiff materials. In particular the JKR theory assumes that adhesion force F_{adh} manifests its presence only within the real contact area (short-range adhesion), and A_r is given by:

$$A_r = \pi\left(\frac{R}{K}\right)^{2/3}\left(F_n + 3\pi\gamma_S R + \sqrt{6\pi\gamma_S R F_n + (3\pi\gamma_S R)^2}\right)^{2/3} \tag{2}$$

where K is the effective elastic modulus of the contact $K^{-1} = 3/4\left[\left(1-\nu_1^2\right)/E_1 + \left(1-\nu_2^2\right)/E_2\right]$ related to the Poisson ratio ν and Young modulus E of surfaces 1 and 2, R the radius of curvature of the (spherical or parabolic) tip and γ_S is the interface energy. We note that for $F_n = -1.5\pi R\gamma_S$ the two surfaces separate when being pulled apart. On the contrary the DMT model assumes that adhesion force F_{adh} manifests its presence also outside the real contact area (long-range adhesion) and at first approximation:

$$A_r = \pi\left(\frac{R}{K}\right)^{2/3}\left(F_n - F_c\right)^{2/3} \tag{3}$$

where F_c represents a constant offset caused by adhesion ($F_c \approx F_{adh}$), related to the interfacial energy γ through the expression $F_c = 2\pi\gamma_S R$. Combining Eqs. (1) and (3), the friction force F_f is given by:

$$F_f = \tau \cdot A_r = C\left(F_n - F_c\right)^{2/3} \tag{4}$$

where $C = \tau \cdot \pi\left(R/K\right)^{2/3}$. It is thus possible to evaluate the friction coefficient for point-contact-like single-asperity friction $\widetilde{C} \equiv C/R^{2/3} = \tau \cdot \pi / K^{2/3}$, which is independent from tip geometry [8,9]. Similar arguments can be applied to the JKR theory combining Eqs. (1) and (2) to obtain:

$$F_f = \tau \cdot A_r = \tau \cdot \pi\left(\frac{R}{K}\right)^{2/3}\left(F_n + 3\pi\gamma_S R + \sqrt{6\pi\gamma_S R F_n + \left(3\pi\gamma_S R\right)^2}\right)^{2/3} \tag{5}$$

To discriminate between the use of the JKR and the DMT theory, the non-dimensional Tabor parameter μ_{Tab} can be estimated [14]:

$$\mu_{Tab} \equiv \left(\frac{9R\gamma_S^{\ 2}}{4K^2 z_0^3}\right)^{1/3} \tag{6}$$

with z_0 representing the equilibrium distance between contact bodies. Tabor's parameter is physically equivalent to the ratio between the normal elastic deformation caused by adhesion (*i.e.* in the absence of applied load) and the spatial range of the adhesion forces themselves. It has been shown that the JKR model holds if $\mu_{Tab} > 5$, whereas the DMT theory is appropriate for systems providing $\mu_{Tab} < 0.1$. Analytical expressions and numerical calculations based on the Maugis-Dugdale theory are used for the intermediate range $0.1 < \mu_{Tab} < 5$ [15].

The agreement of C-AFM friction data with continuum Hertzian models suggests that they capture essential features of dry nanojuction mechanics, yet they have a limited predictive power, since τ is *a priori* unknown for any system of interest. A deeper insight on such aspects can indeed be achieved through atomistic calculations, *e.g.* Molecular Dynamics (MD) simulations, treating contact mechanics and friction for well-defined curved surfaces. Wenning and Muser [16] predicted friction laws for elastic and curved nanocontacts starting from numerical results for flat surfaces: by imposing Hertzian contact mechanics and long-range elasticity into calculations, they demonstrated that disordered and atomically-smooth (amorphous) junctions obey the law $F_f \approx F_n^{2/3}$, while $F_f \propto F_n$ for commensurate contacts and $F_f \approx 0$ for incommensurate interfaces. Of course, we can reasonably model an AFM tip sliding on a hard substrate as an amorphous contact, recovering qualitative agreement with continuum predictions of Eq. (4) and experimental data of Fig. 1. Nevertheless computer simulations provide novel physical basis for the occurrence of the 2/3 power-law. In fact, for flat amorphous surfaces it has been shown that:

$$F_f \propto F_n / \sqrt{A_r} \tag{7}$$

where it appears that friction force is separately affected by F_n, tuning the amplitude of atomistic corrugation barriers, and A_r , controlling the number of involved atoms. Simulations reported in Ref. [16] demonstrate that for curved surfaces $A_r \approx F_n^{2/3}$, which combined with Eq.(1) provides:

$$F_f \approx F_n^{2/3} \tag{8}$$

Analogous results have been recently reported by Luan and Robbins, treating indentation and friction of cylindrical tips against crystalline surfaces [17]. The conceptual advancement of such work is to show that Eq. (1), relating friction force and contact area, breaks down at the nanoscale, since the actual contact area A_r significantly differs from continuum predictions, the shear stress τ is normal-pressure dependent and the total friction force is sensitive to atomic-scale roughness and geometric tip-substrate mismatch. In particular, for amorphous contacts, the local pressure distribution differs significantly from the smooth Hertzian solution but a power-law dependence between F_n and F_f seems to be preserved by arguments similar to those introduced by Ref. [16].

Compared to continuum contact mechanics models, MD simulations clearly enrich the outcome of C-AFM experiments for dry junctions, underlining at the same time the crucial dependence of friction laws of atomic scale details. One possibility to refine continuum mechanics models could be to introduce effective parameters: for example the interface energy γ_S, fitted through continuum models from MD experiments, is found to decrease on increasing atomic-scale roughness. The necessity to adopt atomistic models is nevertheless emerging in a straightforward manner: dry superlubric dynamics is known to occur in C-AFM experiments for crystalline but incommensurate tip-substrate contacts, which is by itself unpredictable to continuum theories.

In agreement with the theoretical insight mentioned above, we underline that the experimental observation of the exponent 2/3 critically depends on the control achieved on the tip shape as well as on substrate roughness. Schwarz *et al.* [8] have pointed out that even the smallest deviations of the tip apex from the spherical shape (appreciated by trasmission electron microscoscopy) can destroy the appearance of the 2/3 power-law on atomically-smooth samples, resulting in power-laws $F_f \approx F_n^m$ with m in the range $0.5-1$. A break down of continuum description is also expected on decreasing contact area to few tens atoms or less: actually, power-laws with $F_f \approx F_n^m$ with $m>1$, have been reported by Socoliuc *et al.* [18] and by Fusco and Fasolino [19], revealing that atomically-sharp tips can show significant deviations from the Hertzian scaling. Moreover, exceptions to the assumption $F_f = \tau \cdot A_r$ have been documented for few systems, namely MoS_2, HOPG, C_{60} monolayers epitaxially grown on GeS(001) [20]: in such case a pressure-dependent shear stress $\tau = \tau_0 + \xi \cdot F_n$ has been introduced, with ξ representing a system specific constant.

3.2 Velocity Dependence of Nanoscale Friction

The velocity dependence of friction has been studied only recently by C-AFM, for sliding velocities going from few nm/s up to several $\mu m/s$. Zwörner *et al.* observed that friction force between Si tips and diamond, graphite or amorphous carbon substrates slightly increases with v [21]. A logarithmic dependence of friction force F_f on v was reported by Gauthier *et al.* and Bouhacina *et al.* for silane molecules and polymers grafted on a silica surface [22,23], by Gourdon *et al.* for Langmuir-Blodgett films [24], by Sills *et al.* for amorphous glassy polystyrene [25]. These results have been often compared with predictions of the phenomenological Eyring's model, a thermally-activated model [26]: it is assumed that the AFM tip is trapped in local minima of the corrugated tip-surface interaction potential and energy barriers, separating neighbour minima, are repeatedly overcome by the tip during sliding. Stochastic tip-substrate interactions induce thermally activated jumps, which reduce friction forces at sufficiently small velocities and provide a logarithmic friction-velocity relationship. In detail, Eyring's model assumes that the height of potential barriers Q increases linearly with applied contact force P while decreases when a shear stress τ is applied. The overall barrier height is $E = Q + P\Omega - \tau\phi_S$, where $P\Omega$ is the compression energy and $\tau\phi_S$ the shear energy; the quantities Ω and ϕ_S are referred to as the

pressure and stress activation volumes respectively and quantify the junction volume (that is the number of molecules) supporting normal and shear forces. Assuming an Arrhenius function to relate the sliding velocity v to a process characteristic velocity v_0 (affected by tip attempt frequency and jump distance) [26], $v = v_0 \exp(-E / k_B T)$, the following relation is deduced for the shear strength:

$$\tau = \frac{k_B T}{\phi_S} \ln\left(\frac{v}{v_0}\right) + \frac{1}{\phi_S}\left(Q + P\Omega\right) \tag{9}$$

Introducing now an effective activation area A'_r, friction and normal forces F_f, F_n are related to the shear strength τ and normal pressure P respectively by $F_f = \tau A'_r$, $F_n = PA'_r$. Hence we have:

$$F_f = k_B T \frac{A'_r}{\phi_S} \ln\left(\frac{v}{v_0}\right) + \frac{1}{\phi_S}\left(A'_r Q + \Omega F_n\right) \tag{10}$$

We note that a logarithmic dependence relates friction force and sliding velocity; however the same equation also predicts a linear dependence of friction force F_f on normal load F_n with a friction coefficient $\mu = \Omega / \phi_S$, which disagrees with the Hertzian power-law dependence reported above. We underline that Sills *et al.* claimed an excellent agreement of their experimental results with the ramp creep model [25], potential barriers being associated to relaxation states of the amorphous polymer and the functional relationship $F_f \propto (\ln v)^{2/3}$ being satisfied.

Recently Tambe and Bhushan explored the velocity dependence of nanoscale friction by means of a commercially-available scanning-tip AFM equipped with a custom calibrated piezostage sample-holder, achieving control over a range of velocities v from 1μm/s to 10mm/s [27]. Experiments conducted on model surfaces, namely silicon oxide, SAM deposited on a Au/Si bilayer, a DLC coating and a Z15-lubricated surface, demonstrated that non-monotonous friction-velocity relationships can be observed, mainly dictated by a system-specific interplay of adhesive, elasto-plastic and thermally-activated contributions dominating different velocities regimes.

3.3 Nanolubrication

Boundary lubrication is a regime of considerable practical importance in which sliding surfaces are separated by at most a few layers of molecules yet an effective friction reduction still exists [28]. Full understanding of this phenomenon demands for a comprehensive characterization of junctions' properties down to their nanoscale features; this emerges especially through surface force apparatus experiments [29], analytical theories [30] and MD simulations [31] attesting a significant dependence of lubricant thinning and shear dynamics on intermolecular forces, atomic-scale roughness, and contaminants. Such complexity seriously affects our predictive capabilities and often limits reproducibility of experimental results. Reports on boundary lubrication for well-defined microcontacts are currently under debate [32]; attempts to probe boundary layers' lubricity within nanosized junctions, as those formed by FFM tips sliding on smooth substrates, are on the contrary quite limited, despite their potential interest for micro/nanofluidic and low friction solutions in technologically advanced devices, as microelectromechanical systems (MEMSs) and their nanoscopic counterpart (NEMS). In 2002 He et al. reported FFM results of efficient nanolubrication by physisorbed simple liquids [33]. Experiments concerned the case of silicon oxide wafers lubricated by octamethylciclotetrasiloxane (OMCTS) and n-hexadecane and probed by nanometric Si tips, sliding with velocities from a few nm/s up to several um/ s under a total compressive load of 100 nN. The authors observed that interfacial liquid structuring reduces kinetic friction, molecular topology ultimately dictating the lubricating properties of boundary layers.

Previous FFM experiments performed under similar working conditions showed, on the contrary, that contact forces in the range of 10–100 nN usually overcome solvation forces associated with interfacial liquid layering, leading to squeeze out of lubricant molecules and poor nanoscale lubricity [34]. Definition of the physical basis of boundary lubrication and experimental details controlling nanoscale lubricity presents indeed a quite challenging task and we note, as a matter of fact, that a comprehensive characterization of contact mechanics and friction laws for lubricated nanocontacts is still missing.

Recently, Buzio et al. [10] provided an attempt to perform similar investigations, starting from the currently established knowledge of nanoscale friction phenomena (see above). AFM measurements in liquid were performed with the Si tips (curvature radius $R \approx 40\text{nm}$) fully immersed in oils and placed in contact with carefully prepared substrates (glass and quartz). Average friction vs load curves are shown in Fig. 2 for OMCTS and squalane, a branched alkane: experimental data are plotted with respect to the total normal load F_n (adhesive plus externally applied compressive load) and compared to the DMT fits of Fig. 1, that appear now shifted on the horizontal axis by an amount $-F_c$: this is done to assure the same origin to dry and lubricated friction curves and highlight friction differences.

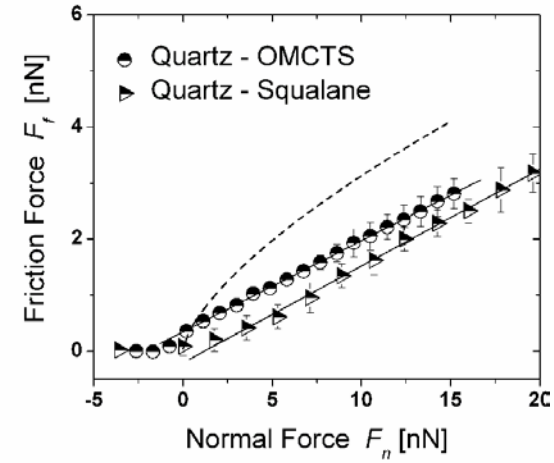

Fig. 2 Average friction vs load curves acquired on quartz lubricated by OMCTS and squalane: they follow a linear relationship, in agreement with Amontons' law and MD simulations (see text). Adhesion appears considerably reduced (adapted from [10]).

It appears that the Amontons' law relates F_f and F_n, in detail $F_f = \mu F_n + F_0$ (the parameter F_0 was intentionally added to account for small deviations at low loads). With respect to dry air, friction forces on quartz are reduced of 30% by OMCTS and 35% by squalane for $F_n \approx 5\text{nN} - 20\text{nN}$, proving a dependence of lubricated friction on molecular topology. By linearly fitting experimental data the friction coefficients $\mu_{OMCTS}^{Quartz} = 0.16 \pm 0.01$ and $\mu_{Squalane}^{Quartz} = 0.17 \pm 0.01$ were obtained. Buzio *et al.* separately verified that such linearity could be extended up to $F_n \approx 40\text{nN}$ without affecting system reproducibility. Qualitatively similar results were observed for glass: in such case however friction reduction due to lubrication was of 10% only; the friction coefficients were $\mu_{OMCTS}^{Glass} = 0.22 \pm 0.01$ and $\mu_{Squalane}^{Glass} = 0.26 \pm 0.01$.

The most striking evidence of above results is that a quantitative reduction of friction occurs in FFM experiments due to weakly-bounded layers: this is accompanied by the appearance of the Amontons' law, with friction coefficients related to the substrate and molecular properties. Such behaviour cannot be easily accounted for by Eqs.(1) and (2) but an *atomistic picture* is necessary to explain the main part of our findings. Common sense dictates that the possibility to achieve a liquid-mediated sliding friction relies on the load-bearing capacity of boundary layers, estimated in terms of their squeeze force, the maximum force that layers can sustain before being expelled from the contact. As recently observed within realistic MD simulations [16] squeeze force significantly depends on loading and shear conditions as well as on the molecules-surface interaction potential, which in turn is affected by molecular topology,

substrate symmetry and nanoroughness: these aspects crucially affect the magnitude of squeeze force, they tune nanoscale lubricity and ultimately impart atomic-scale character to boundary lubrication. According to MD calculations [16,31], Eqs. 4,8 describe friction between bare elastic nanocontacts; when physisorbed atoms or molecules exist and large contact pressures are applied (~0.1GPa, as in typical FFM experiments), the tip can partially penetrate the last boundary layer. Such composite interface is however not equivalent to the dry case, because normal pressure is sustained at the bare wall-wall interface as well as further outside, where wetting liquid molecules decrease the effective distance between tip and surface: simulations reveal that these "outskirts" carry load and contribute significantly to the net friction force according to the linear law $F_f = \mu F_n$. Thus the total friction force results from the superposition of a *dry* contribution, acting at the very end of the tip (and scaling as Eq. 8), and a *lubricated* contribution (satisfying Amontons' law), localized around the dry region: the friction-load law comes out from the balance of both effects and can be of linear or sublinear type ($F_f \propto F_n^{\beta}$ with $2/3 \le \beta \le 1$). This shows that both squeeze pressure and wetting properties play a pivotal role in defining friction laws for nanolubrication. For the reported FFM experiments, Buzio *et al.* assumed that lubricant molecules were dominating junction dynamics and dictating the appearance of the Amontons' law. A quantitative analysis of nanolubrication and its velocity dependence, based on the Eyring model, is reported in Ref. [10].

4. Conclusions

We summarized the phenomenology of nanoscale friction, as measured by AFM, and provided continuum mechanics and atomistic arguments to describe the load and velocity dependences. The case of lubricated nanocontacts deserves special attention for his potential impact on MEMS and NEMS technology.

Recent experiments on nanolubrication show that: 1) sliding friction is quantitatively reduced in liquid environment with respect to dry air provided that AFM tips curvature radii are of few tens nanometers; 2) nanolubrication is correlated to the appearance of the Amontons' law, with kinetic friction coefficients in the range 0.16 - 0.26 according to the studied liquid and interface roughness. These experimental findings are in qualitative agreement with MD simulations suggesting Amontons' law to be a signature of liquid-mediated nanofriction. Plastic deformation of load-bearing boundary layers is suggested to be the most likely explanation for energy dissipation.

Nanoscale lubrication needs therefore to be related to atomic scale system properties: once again this point emphasizes the complexity and potential developments of this field.

Acknowledgements The support by MIUR-FIRB project "NANOMED" is gratefully acknowledged.

References

[1] G. Binnig, C. E. Quate, Ch. Gerber, Physical Review Letters 56, 930 (1986).
[2] E. Meyer and H. Heinzelmann in R. Wiesendanger and H. J. Guntherods Eds., Scanning Tunneling Microscopy II, Springer - Verlag, Berlin Heidelberg (1992), Chapter 4.
[3] B. Bhushan and H. Fuchs Eds., Applied Scanning Probe Methods I-II, Springer - Verlag, Berlin Heidelberg (2005).
[4] S. Morita, R. Wiesendanger and E. Meyer Eds., Non-Contact Atomic Force Microscopy, Springer - Verlag, Berlin Heidelberg (2004).
[5] B. Cappella, G. Dietler, Surface Science Reports 34, 1 (1999).
[6] R. Garcia, R. Perez, Surface Science Reports 47, 197 (2002).
[7] H. J. Butt, B. Cappella, M. Kappl, Surface Science Reports 59, 1 (2005).
[8] U. D. Schwarz, O. Zwoerner, P. Koester, R. Wiesendanger, Physical Review B 57, 6987 (1997).
[9] R. Buzio, E. Gnecco, C. Boragno, U. Valbusa, Carbon 40, 883 (2002).
[10] R. Buzio, C. Boragno, U. Valbusa, The Journal of Chemical Physics 125, 094708 (2006).
[11] W. N. Unertl, Journal of Vacuum Science and Technology A **17**, 1779 (1999).

[12] K. L. Johnson, K. Kendall, and A. D. Roberts, Proceedings of the Royal Society London A 324, 301 (1971).
[13] B. V. Derjaguin, V. M. Muller and Y. P. Toporov, Journal of Colloids and Interface Science 53, 314 (1975).
[14] J. A. Greenwood, Proc. R. Soc. Lond. A 453, 1277 (1997).
[15] D. Maugis, Journal of Colloids and Interface Science 150, 243 (1992);
[16] L. Wenning and M. Muser, Europhysics Letters 54, 693 (2001).
[17] B. Luan and M. O. Robbins, Nature 435, 929 (2005).
[18] A. Socoliuc, R. Bennewitz, E. Gnecco, and E. Meyer, Physical Review Letters 92, 134301 (2004).
[19] C. Fusco, A. Fasolino, Applied Physics Letters 84, 699 (2004).
[20] U.D. Schwarz, W. Allers, G. Gensterblum, R. Wiesendanger, Physical Review B 52, 14976 (1995).
[21] O. Zwörner, H. Hölscher, U. D. Schwarz and R. Wiesendanger, Applied Physics A 66, S263 (1998).
[22] S. Gautier, J. P. Aimé, T. Bouhacina, A. J. Attias, B. Desbat, Langmuir 12, 5126 (1996).
[23] T. Bouhacina, J. P. Aimé, S. Gautier, D. Michel, V. Heroguez, Physical Review B 56, 7694 (1997).
[24] D. Gourdon, N. A. Burnham, A. Kulik, E. Dupas, F. Oulevey, G. Gremaud, D. Stamou, M. Liley, Z. Dienes, H. Vogel, C. Duschl, Tribology Letters 3, 317 (1997).
[25] S. Sills, R. M. Overney, Physical Review Letters 91,095501 (2003).
[26] H. Eyring, The Journal of Chemical Physics 4, 283 (1936).
[27] N. S. Tambe and B. Bhushan, J. Phys. D: Applied Physics 38, 764 (2005).
[28] B. N. J. Persson, Sliding Friction: Physical Principles and Applications, Springer-Verlag, Heidelberg, (2000).
[29] R. G. Horn and J. Israelachvili, The Journal of Chemical Physics 75, 1400 (1981).
[30] S. Zilberman, B. N. J. Persson, A. Nitzan, The Journal of Chemical Physics 115, 11268 (2001).
[31] I. M. Sivebaek, V. N. Samoilov, B. N. J. Persson, The Journal of Chemical Physics 119, 2314 (2003).
[32] Y. Zhu, S. Granick, Langmuir 19, 8148 (2003).
[33] M. He, A. S. Blum, G. Overney, and R. M. Overney, Physical Review Letters 88, 154302-1 (2002).
[34] V. N. Koinkar, B. Bhushan, Journal of Applied Physics 79, 8071 (1996).